Vibrational Modes of Ubiquinone in Cytochrome bo_3 from *Escherichia coli* Identified by Fourier Transform Infrared Difference Spectroscopy and Specific ^{13}C Labeling†

Petra Hellwig,*,‡ Tatsushi Mogi,§ Farol L. Tomson,|| Robert B. Gennis,|| Jun Iwata,⊥ Hideto Miyoshi,⊥ and Werner Mäntele‡

Institut für Biophysik der Johann-Wolfgang-Goethe-Universität, Theodor-Stern-Kai 7, Haus 74, 60590 Frankfurt/M., Germany, Department of Biological Sciences, Graduate School of Science, University of Tokyo, Hongo, Bunkyo-ku, Tokyo 113-0033, Japan, Department of Biochemistry, University of Illinois, 600 South Mathews Avenue, Urbana, Illinois, and Division of Applied Life Sciences, Graduate School of Agriculture, Kyoto University, Kitashirakawa, Sakyo-ku, Kyoto 606-8502, Japan

Received June 2, 1999; Revised Manuscript Received August 19, 1999

ABSTRACT: In this study we present the infrared spectroscopic characterization of the bound ubiquinone in cytochrome bo_3 from *Escherichia coli*. Electrochemically induced Fourier transform infrared (FTIR) difference spectra of ΔUbiA (an oxidase devoid of bound ubiquinone) and ΔUbiA reconstituted with ubiquinone 2 and with isotopically labeled ubiquinone 2, where ^{13}C was introduced either at the 1- or at the 4-position of the ring (C═O groups), have been obtained. The vibrational modes of the quinone bound to the discussed high-affinity binding site (Q_H) are compared to those from the synthetic quinones in solution, leading to the assignment of the C═O modes to a split signal at 1658/1668 cm^{-1}, with both carbonyls similarly contributing. The FTIR spectra of ΔUbiA reconstituted with the labeled quinones indicate an essentially symmetrical and weak hydrogen bonding of the two C═O groups from the neutral quinone with the protein and distinct conformations of the 2- and 3-methoxy groups. Perturbations of the vibrational modes of the 5-methyl side groups are discussed for a signal at 1452 cm^{-1}. Only negligible shifts of the aromatic ring modes can be reported for the reduced and the protonated form of the quinone. Alterations of the protein upon quinone binding are reflected in the electrochemically induced FTIR difference spectra. In particular, difference signals at 1640−1633 cm^{-1} and 1700−1670 cm^{-1} indicate variations of β-sheet secondary structure elements and loops, bands at 1706 and 1678 cm^{-1} are tentatively attributed to individual amino acids, and a difference signal a 1540 cm^{-1} is discussed to reflect an influence on C═C modes of the porphyrin ring or on deprotonated propionate groups of the hemes. Further tentative assignments are presented and discussed. The ^{13}C labeling experiments allow the assignment of the vibrational modes of a bound ubiquinone 8 in the electrochemically induced FTIR difference spectra of wild-type bo_3.

Cytochrome bo_3 from *Escherichia coli* is a member of the heme−copper terminal oxidase superfamily and catalyzes the two-electron oxidation of ubiquinol 8 (UQ_8H_2)[1] and the four-electron reduction of dioxygen, which are coupled to vectorial translocation of protons across the cytoplasmic membrane by a pump mechanism (*1*−*3*). The presence and cooperation of two quinone/quinol binding sites are discussed for the oxidation of quinols and provide a unique feature to the electron input site of eubacterial quinol oxidases (*3*). Purified enzyme contains a tightly bound UQ_8 (*4*), which can be stabilized as a ubisemiquinone radical during enzymatic turnover (*5*, *6*). The bound UQ_8 at the high-affinity quinone binding site (Q_H) mediates electron transfer from the low-affinity quinol oxidation site (Q_L) in subunit II to the low-spin heme *b* in subunit I (*3*, *4*, *7*−*10*). Sato-Watanabe et al. (*4*, *5*, *9*, *10*) postulated that the Q_H site serves as a transient electron reservoir for the two-electron supply from the Q_L site and gates electron transfer, allowing sequential one-electron transfer from the Q_L site to heme *b*. The location of the Q_H site remains to be examined, whereas the Q_L site was proposed to be present in the C-terminal hydrophilic domain of subunit II by photoaffinity cross-linking (*7*, *11*) and mutagenesis studies (*10*, *12*).

Infrared spectroscopy is a sensitive method used to study the structural changes that accompany the redox reaction of the quinones, as previously shown for the vibrational modes

† This work was supported in part by DFG (Ma1054/17-1 and 17-2 to W.M.); by Grants-in-Aid for Scientific Research on Priority Areas (08249106 to T.M., 10129213 to H.M.) and for Scientific Research (A) (10358016 to T.M.) from the Ministry of Education, Science, Sports and Culture, Japan; and by a grant (DEFG-02-87ER13716 to R.B.G.) from the U.S. Department of Energy.

* To whom correspondence should be addressed: email hellwig@biophysik.uni-frankfurt.de; Tel 49-69-6301-5835; Fax 49-69-6301-5838.

‡ Institut für Biophysik der Johann-Wolfgang-Goethe-Universität.

§ University of Tokyo.

|| University of Illinois.

⊥ Kyoto University.

[1] Abbreviations: FTIR, Fourier transform infrared; SHE′, standard hydrogen electrode (pH 7); Q_H, the high-affinity quinone binding site; Q_L, the low-affinity quinol oxidation site; ΔUbiA, the wild-type cytochrome bo_3 purified from a ubiquinone biosynthesis mutant; UQ, ubiquinone; DM, *n*-dodecyl β-D-maltoside.

10.1021/bi991267h CCC: $18.00
Published on Web 10/15/1999

of the quinones in the bacterial reaction center in light-induced FTIR difference spectra (*13*−*18*). The vibrational modes of the quinones in their different redox and protonation states can serve as reporter groups for steric and energetic factors such as hydrogen bonding, polar interactions, and distortion of ring and substituents. As a common characteristic feature ubiquinones have a long isoprenyl side chain that may have a structural role in anchoring the quinone headgroup to the specific binding sites. In addition to this interaction, hydrogen bonds can be expected between the carbonyls of the quinone and proton-donating groups from amino acids. Structure−function studies on cytochrome bo_3 with synthetic UQ_2 derivatives revealed that the 2-methoxy and 5-methyl groups are required for the catalytic turnover (*19*). One of the two π-electron systems in the 6-isoprenyl tail is required for high-affinity binding of UQ_2H_2, while the presence of the methyl branch and the location of the π-electron systems are not strictly recognized by the Q_L site (*20*). Studies with benzoquinones and ubiquinone-related inhibitors indicated that one of the quinone C═O groups is structurally more important for the binding in the Q_L site (*21*). Such hydrogen bonds between the C═O or C−O−H groups of ubiquinols and proton donating or accepting groups must exist for binding and catalytic turnover of ubiquinols at the Q_L and Q_H sites of cytochrome bo_3.

Previously, isotopically labeled quinones were used to identify the quinone modes of the Q_A and Q_B in the bacterial reaction center and characterize their binding sites (*14*−*16*). In this study, we synthesized UQ_2 derivatives selectively labeled with ^{13}C at the 1- or the 4-position of the quinone ring ([1-^{13}C]UQ_2 and [4-^{13}C]UQ_2; see inset in Figure 1) and applied a similar approach to the bound ubiquinone at the Q_H site of cytochrome bo_3 in order to probe its molecular environment. Vibrational modes from the bound quinone in the electrochemically induced FTIR difference spectra were separated by double difference spectroscopy from the protein contributions on the basis of those of the cytochrome bo_3 devoid of bound ubiquinone (ΔUbiA) reconstituted with either [^{12}C]UQ_2, [1-^{13}C]UQ_2, or [4-^{13}C]UQ_2. Alterations on the protein modes upon the ubiquinone binding and symmetric or unsymmetrical binding of the ubiquinone and hydrogen bonding are discussed.

MATERIALS AND METHODS

Sample Preparation. UQ_2 selectively labeled with ^{13}C at the 1- or the 4-position of the quinone ring (i.e., [1-^{13}C]UQ_2 or [4-^{13}C]UQ_2) was synthesized from specific ^{13}C-labeled methylsuccinic acid by the procedure of van Liemt et al. (*22*). ^1H and ^{13}C NMR spectra of the products were identical to those in ref *22* and showed a ^{13}C content of 97% or better. Absorption spectra of the UQ_2 analogues were determined in acetonitrile-d_3 (Merck) at approximately 75 mM. For the electrochemical analysis, the synthetic UQ_2 analogues were solubilized in 50 mM phosphate buffer (pH 7), 100 mM KCl, and 0.1% sucrose monolaurate at a concentration of approximately 1 mM.

Wild-type bo_3 enzyme with a bound UQ_8 was purified according to the method described by Rumbley et al. (*24*). The following changes were made to the purification procedure: 0.1% SOL-grade *n*-dodecyl β-D-maltoside (DM; Anatrace, Inc., Maumee, Ohio) was used for solubilization and the same detergent was used at 0.1% concentration for the remaining purification steps. The protein was eluted by a buffer of 50 mM K_2HPO_4, 100 mM imidazole, and 0.1% DM, pH 8.0. The protein was dialyzed against a buffer containing 200 mM phosphate, 100 mM KCl, and 0.1% DM, pH 7.0. Glycerol (5%) was added after dialysis to protect the enzyme during storage at −80 °C.

Cytochrome bo_3 without a bound UQ_8 (ΔUbiA) was isolated from the ubiquinone biosynthesis mutant MU1227/pMFO4 (*cyo*$^+$ *cyd*$^+$Δ*UbiA*/*cyo*$^+$) as described previously (*4*) and stored in 50 mM Tris-HCl buffer (pH 7.4) containing 0.1% sucrose monolaurate (Mitsubishi-Kagaku Foods Co., Tokyo). For reconstitution with the synthetic UQ_2 analogues, 25 nM ΔUbiA was incubated overnight on ice with an equimolar amount of UQ_2 in 0.5 mL of 50 mM Tris-HCl (pH 7.4) containing 0.1% sucrose monolaurate and concentrated to about 0.25 mM by ultrafiltration with Centricon 100. The reconstitution of the Q_H site was confirmed by the Soret peak shift from 412 to 409 nm, and the enzymes were used without further purification due to a relatively higher K_d value (about 2 μM) for ubiquinones (*9*, *21*).

For electrochemistry the protein samples were concentrated to approximately 0.5 mM by using Microcon ultrafiltration cells (Millipore) and dispersed in 200 mM phosphate buffer (pH 7) containing 100 mM KCl and 0.1% DM.

Electrochemistry. The ultra-thin-layer spectroelectrochemical cell for the UV/vis and IR was used as previously described (*25*). Sufficient transmission in the 1800−1000 cm^{-1} range, even in the region of strong water absorbance around 1645 cm^{-1} (minimum 15%), was achieved with the cell path length set to 6−8 μm. The gold grid working electrode was chemically modified by a 2 mM cysteamine solution as reported before (*26*). To accelerate the redox reaction, 16 different mediators were added as reported in ref *26* (except *n*-methylphenazonium methosulfate and *n*-ethylphenazonium sulfate, but adding neutral red; E_m −307 mV vs SHE′) to a final concentration of 45 μM each. At this concentration, and with the cell path length below 10 μm, no spectral contributions from the mediators in the vis and IR range could be detected in control experiments with samples lacking the protein, except for the PO modes of the phosphate buffer between 1200 and 1000 cm^{-1}. For the experiments with synthetic quinones, the gold electrode was used unmodified and no mediators were added. Approximately 5−6 μL of the protein solution was sufficient to fill the spectroelectrochemical cell. Potentials quoted with the data refer to the Ag/AgCl/3 M KCl reference electrode; add +208 mV for SHE′ (pH 7) potentials.

Spectroscopy. FTIR and UV/vis difference spectra as a function of the applied potential were obtained simultaneously from the same sample with a setup combining an IR beam from the interferometer (modified IFS 25, Bruker, Germany) for the 4000−1000 cm^{-1} range and a dispersive spectrometer for the 400−900 nm range. First, the protein was equilibrated with an initial potential at the electrode, and single-beam spectra in the IR range were recorded. A potential step toward the final potential was then applied, and single-beam spectra of this state were again recorded after equilibration. Difference spectra as presented here were then calculated from the two single-beam spectra, with the initial single-beam spectrum taken as reference. Double difference spectra have been calculated by interactive

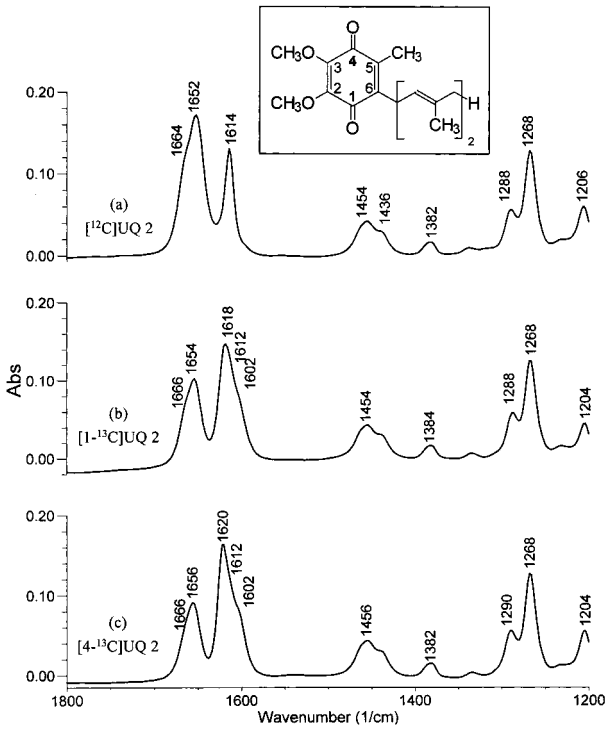

FIGURE 1: Infrared absorbance spectra of [^{12}C]UQ_2 (a), of [1-^{13}C]-UQ_2 (b), and of [4-^{13}C]UQ_2 (c) in acetonitrile-d_3. The contributions of the solvent were interactively subtracted. The inset shows the structural formula of ubiquinone 2 (2,3-dimethoxy-5-methyl-6-diprenyl-1,4-benzoquinone).

subtraction of two difference spectra, weighted because of differences in the sample concentration and cell path length. No smoothing or deconvolution procedures were applied. The equilibration for the applied potential generally took less than 6 min under the conditions (protein concentration, electrode modification, mediators) reported for the potential step from −0.5 to 0.5 V. The ΔUbiA enzyme, however, showed significantly higher equilibration times as compared to the wild-type enzyme (10−13 min). Typically, 128 interferograms at 4 cm^{-1} resolution were coadded for each single-beam IR spectrum and Fourier transformed by using triangular apodization. A total of 5−15 difference spectra were usually averaged. The noise level in the difference spectra was estimated to be around (25−50) × 10^{-6} absorbance units and is slightly higher in regions of strong absorbance of the sample at 1650 cm^{-1} (amide I and water OH modes). For the absorbance spectra a cell consisting of two CaF_2 windows with a path length of 7.8 μm was used; 0.6 μL of the sample was sufficient to fill the cell. The contributions of the solvent were interactively subtracted.

RESULTS AND DISCUSSION

Infrared Absorbance Spectra of the Quinones in Vitro. Figure 1a shows the infrared absorbance spectra of unlabeled ubiquinone 2 ([^{12}C]UQ_2) in acetonitrile-d_3. The inset depicts the molecular structure of UQ_2 and the numbering of the C-atoms in the quinone ring. The split C═O modes of [^{12}C]-UQ_2 (Figure 1a) can be identified at 1664 and 1652 cm^{-1} and the C═C modes at 1614 cm^{-1}. At 1454, 1436, and 1382 cm^{-1}, the $\delta(CH_2)$ and $\delta(CH_3)$ vibrations of the chain, the 5-methyl group, and the 2- and 3-methoxy groups are located. At 1288 and 1268 cm^{-1}, the signals of the C−OCH_3 vibrations of the 2- and 3-methoxy groups are present. These assignments are in line with those described in Breton et al. (*16*).

Figure 1b,c shows the absorbance spectra of [1-^{13}C]UQ_2 (b) and of [4-^{13}C]UQ_2 (c). The $\delta(CH_2)$ and $\delta(CH_3)$ vibrations of the chain, the 5-methyl group, and the 2- and 3-methoxy groups at 1454, 1436, and 1382 cm^{-1}, as well as the C−OCH_3 vibrations of the 2- and 3-methoxy groups at 1288 and 1268 cm^{-1} are essentially unaffected. The carbonyl bands at 1664 and 1652 cm^{-1} decrease in intensity, accompanied by the appearance of a new band at 1618 cm^{-1} for C1═O (Figure 1b) or at 1620 cm^{-1} for C4═O (Figure 1c). The shift of 38 cm^{-1} for ^{13}C1═O and of 36 cm^{-1} for ^{13}C4═O is in line with a simple reduced mass estimation (harmonic oscillator approximation) of 37 cm^{-1} for ^{12}C → ^{13}C substitution expected for an isolated C═O mode. The signals at 1664 and 1654/1656 cm^{-1} are decreased but both still present. This indicates that both C═O groups contribute to these signals with split modes. The influence of the ^{13}C labeling at the C═O groups on the C═C modes is revealed by the appearance of a signal at 1602 cm^{-1} accompanied by the decrease of the signal at 1614 cm^{-1}. The strong coupling of the C═C to the C═O modes results in this complex picture and the C═C modes are similarly altered by the labeling at the C1 or C4 position.

The same effects were observed and discussed before for site-specifically ^{13}C-labeled UQ_1 and UQ_3 (*14*, *15*). The shifts of the C═C and the C═O modes were explained by the strong coupling in the system. The splitting of the C═O modes to 1664 and 1652 cm^{-1} for each carbonyl group was attributed to different conformations of the two adjacent methoxy groups and their influence on the C═O vibrational energy. Two ubiquinone conformers have been recently reported to be favored on the basis of semiempiric calculations and IR spectra (*27*, *28*). In one of the discussed forms, one methoxy group adapts the conformation of a free methoxy group, and in the second, that of a hindered methoxy group. Two subconformers are possible, the methoxy group at C2 or C3 being hindered. In the other conformer both methoxy groups are hindered. The first conformer was shown to dominate at room temperature in solution (*27*). However, a low rotational barrier and an interconversion of both forms is expected in solution. A discussion of the conformer present in the cytochrome bo_3 and the resulting different electrochemical properties will be given below.

Electrochemically Induced FTIR Difference Spectra of the Synthetic Quinones. The oxidized minus reduced FTIR difference spectra of [^{12}C]UQ_2 (a), of [1-^{13}C]UQ_2 (b), and of [4-^{13}C]UQ_2 (c) in aqueous phosphate buffer containing 0.1% sucrose monolaurate are shown in Figure 2. The spectra presented here show the potential step from −0.5 to 0.5 V (vs Ag/AgCl), the positive signals correlate with the neutral quinone and the negative with the reduced and protonated form, UQ_2H_2. Fully reversible reactions were observed (data not shown). The signals of the neutral quinone essentially correspond to the modes observed in the absorbance spectra (Figure 1). Only a negligible influence of the solvent on the signals can be reported for the C═O and C═C modes. The C−O modes of the methoxy groups show a downshift of 4 cm^{-1} with respect to their absorption in acetonitrile-d_3. This may be attributed to the different dielectric constant of the solvents (81 vs 38.8).

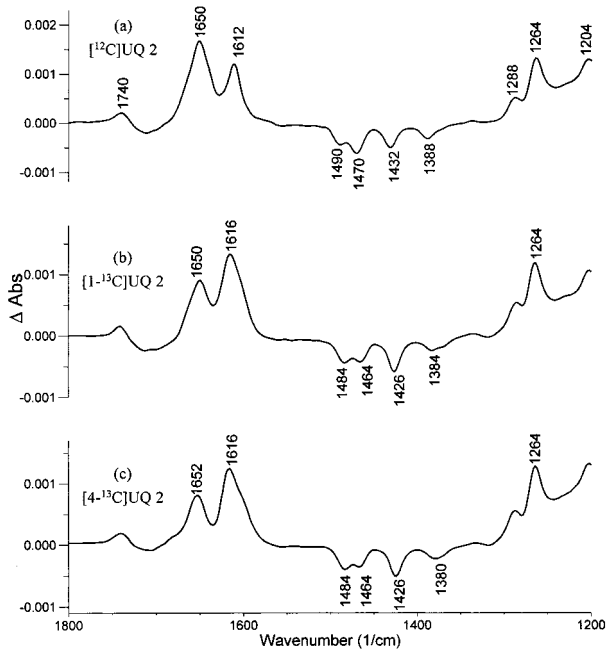

FIGURE 2: Oxidized minus reduced FTIR difference spectra of [^{12}C]-UQ_2 (a), of [1-^{13}C]UQ_2 (b), and of [4-^{13}C]UQ_2 (c) in aqueous phosphate buffer containing 0.1% sucrose monolaurate for a potential step from −0.5 to 0.5 V.

The negative signals at 1490, 1470, 1432, and 1388 cm^{-1} of the unlabeled [^{12}C]UQ_2 (Figure 2a) can be attributed to reorganizations of the quinone ring. However, precise assignments of the quinol modes are not clear yet. For the conditions used here (pH 7, aqueous solution, potential applied, and the equilibration of the sample over several minutes), the full reduction and protonation of the quinone is expected. The signal at 1490 cm^{-1} was previously assigned to the C−O mode of the semiquinone anion form (*29*). This assignment does not seem likely, since the semiquinone anion form is not stable under the conditions examined in aqueous solution, yet the mode at 1490 cm^{-1} is present.

At 1740 cm^{-1} an unusual difference signal can be observed, which is not due to a ubiquinone vibrational mode (see above). We attribute this signal to the detergent used here to solubilize the quinone, sucrose monolaurate, reflecting the reorganizations of a C═O group of the detergent oriented toward the quinone and affected by the quinone redox transition. In control measurements of the buffer/detergent system lacking the quinone, the signal is not present, nor in spectra of the quinone in organic solvents.

In the spectral region below 1350 cm^{-1} a shift of the baseline is observable, caused by the broad shoulder of the difference signals of the P═O modes from the phosphate buffer used (*26*). This feature is observed in all spectra presented here.

Electrochemically Induced FTIR Difference Spectra of ΔUbiA and of ΔUbiA Reconstituted with Labeled Quinones. Figure 3a presents the oxidized-minus-reduced FTIR difference spectra of ΔUbiA for a potential step from −0.5 to 0.5 V in the spectral range from 1800 to 1200 cm^{-1}. ΔUbiA is the wild-type cytochrome bo_3 from *E. coli* purified from a ubiquinone biosynthesis mutant devoid of the bound UQ_8 at the Q_H site. In the electrochemically induced FTIR difference spectra, contributions from the reorganization of hemes *b* and o_3, secondary structure elements, and individual amino

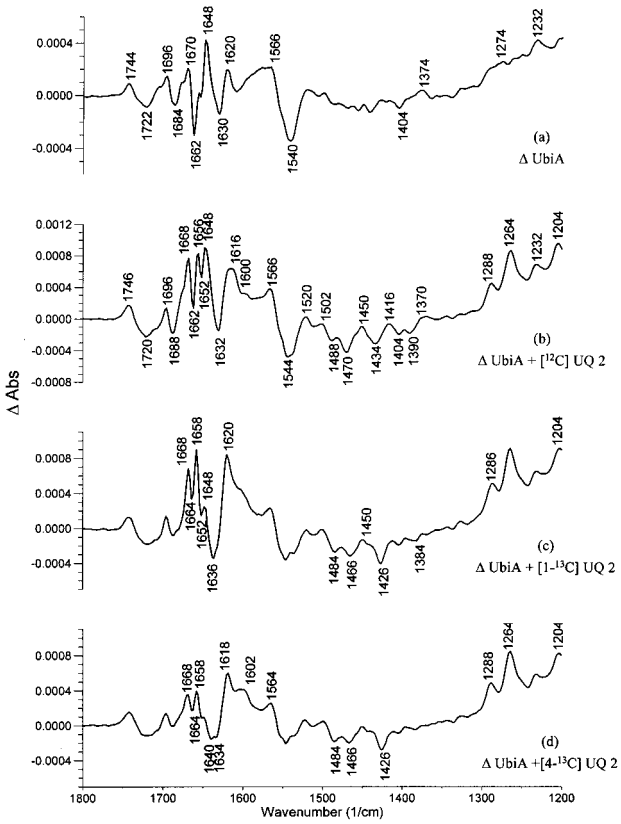

FIGURE 3: Oxidized minus reduced FTIR difference spectra of ΔUbiA (a) and of ΔUbiA oxidase reconstituted with [^{12}C]UQ_2 (b), [1-^{13}C]UQ_2 (c), and [4-^{13}C]UQ_2 (d) for a potential step from −0.5 to 0.5 V.

acids concomitant with electron transfer and coupled proton translocation can be expected. In the amide I range (1690−1620 cm^{-1}) difference signals at 1670, 1662, 1648, and 1630 cm^{-1} indicate absorbance changes of C═O modes caused by small alterations in the polypeptide backbone upon the redox process and possible contributions from C═O modes of individual amino acid side chains (Asn and Gln). In the amide II range (1570−1520 cm^{-1}), coupled CN stretching and NH bending modes are expected. Vibrational modes from aromatic amino acids and heme C═C modes from the porphyrin ring, for example at 1540 cm^{-1}, are conceivable. Antisymmetric COO^- modes from deprotonated heme propionates and Asp or Glu side chains, caused by protonation/deprotonation of COOH groups, may also contribute here. In the spectral region above 1680 cm^{-1}, signals from protonated heme propionates, and above 1710 cm^{-1}, from protonated Asp and Glu, are likely. The difference signals at 1744/1722 cm^{-1} have been assigned in a combined IR/mutagenesis study to the COOH mode of Glu286 (*30*, *31*). Lübben et al. (*32*) also have proposed an assignment for this mode to Glu286, however, for signals at 1745/1735 cm^{-1} and observing a different shift for case of the Glu286Asp mutant enzyme. The reason for the discrepancy of about 13 cm^{-1} and the different effect of the mutant is unclear (compare ref *31*). In a study on the cytochrome *c* oxidase from *Paracoccus denitrificans* with the method used here, the analogous signals at 1746/1734 cm^{-1} were attributed to the COOH modes of Glu278 (*26*).

Oxidized minus reduced FTIR difference spectra of ΔUbiA and ΔUbiA reconstituted with [^{12}C]UQ_2, [1-^{13}C]UQ_2, and [4-^{13}C]UQ_2 (Figure 3) should reflect the redox reactions

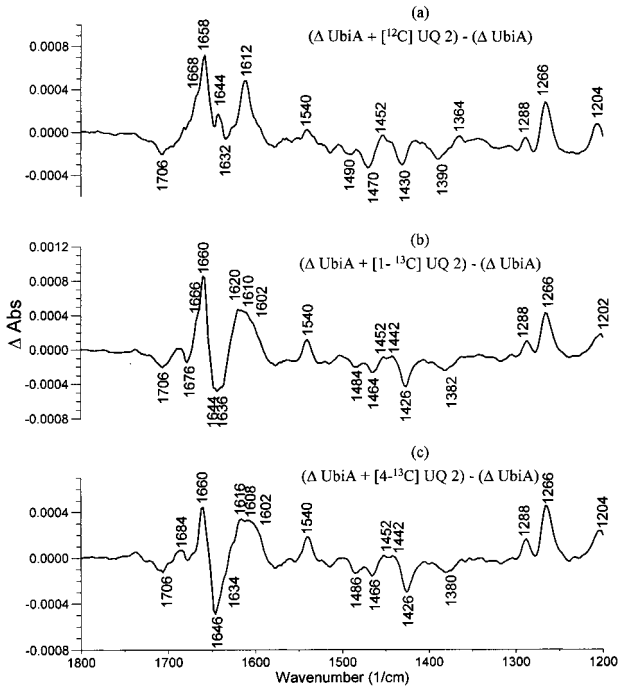

FIGURE 4: Double difference spectra calculated by interactive subtraction of the electrochemically induced FTIR difference spectra of ΔUbiA reconstituted with UQ_2 (Figure 3b−d) from the electrochemically induced FTIR difference spectra of ΔUbiA (Figure 3a). The double difference spectra present the contributions of $[^{12}C]UQ_2$ (a), $[1\text{-}^{13}C]UQ_2$ (b), and $[4\text{-}^{13}C]UQ_2$ (c) bound in the discussed Q_H site and reorganizations of the protein site.

of the bound UQ_2 analogues and the protein structural changes upon their binding. To identify the quinone and protein modes, double difference spectra (Figure 4) were calculated by interactive subtraction of the electrochemically induced FTIR difference spectra of ΔUbiA reconstituted with the UQ_2 analogues (Figure 3b−d) from that of ΔUbiA (Figure 3a).

C═O Modes of the Neutral Bound Quinone. The C═O modes of $[^{12}C]UQ_2$ show a broad signal at 1650 cm^{-1} with a shoulder at 1664 cm^{-1} in aqueous solution (Figure 2a) and a much sharper signal at 1658 cm^{-1} with a small shoulder at 1668 cm^{-1} in the protein-bound state (Figure 4a). The change in the bandwidth clearly indicates the fixed orientation and the restriction of conformational flexibility of the ubiquinone upon binding. The frequencies of the C═O modes are close to the ones observed in aqueous solution (1664 and 1650 cm^{-1}, see Figure 2), where fluctuating binding partners are present. Strong hydrogen bonding of the carbonyl group by a specific hydrogen bond would lead to a large downshift of the C═O mode. Thus, the observed frequencies of the C═O modes for the ubiquinone bound in the protein site reveal relatively weak hydrogen bonding with the binding pocket.

The difference spectrum of UbiA reconstituted with $[1\text{-}^{13}C]$-UQ_2 (Figure 3c) and the double difference spectrum in Figure 4b allow us to identify the $^{12}C4{=}O$ mode at 1660 cm^{-1} with a shoulder at 1666 cm^{-1}. The $^{13}C1{=}O$ mode is observable at approximately 1620 cm^{-1}; however, negative signals at 1644−1636 cm^{-1} make a clear determination of the maximum difficult. By use of ΔUbiA reconstituted with $[4\text{-}^{13}C]$-UQ_2 (Figure 3d and 4c), the $^{12}C1{=}O$ mode was similarly identified at 1660 cm^{-1} without a significant shoulder. The $^{13}C4{=}O$ mode can be seen at ∼1616 cm^{-1}, but a broad negative band at 1644−1636 cm^{-1} makes a clear determination of the maximum difficult.

In the absorbance spectra (Figure 1b,c) and in the electrochemically induced FTIR difference spectra (Figure 2b,c) presented for the quinones in vitro, both carbonyls contribute similarly; the signals at 1664/1652 cm^{-1} both decrease upon site-specific ^{13}C labeling. In the double difference spectra in Figure 4b, the signal at 1666/1660 cm^{-1} is not that strongly decreased compared to the spectra of the free compound (Figure 2b). This may indicate a change in the extinction coefficient for the C4═O, caused by a small perturbation in the binding pocket and clearly showing that the UQ_2 observed here is associated with the protein. As discussed above, different conformers of the adjacent methoxy groups in ubiquinone result in the split C═O modes. The comparison of the double difference spectra in Figure 4a−c to the extinction coefficients of the C═O groups for the different conformers calculated in Burie et al. (*27*) provides supporting evidence for the 3-methoxy group close to C4═O in UQ_2 to be in plane with the ring and the 2-methoxy group to be oriented out of the ring plane. Furthermore, the binding of the two C═O groups of the neutral quinone with the protein appears to be essentially symmetrical. We keep in mind that the protein environment, the hydrogen bonding, and the local dielectric constant may additionally influence extinction coefficients.

The conformers of the ubiquinone could have different midpoint potentials (*33*). The midpoint potential should be higher for the conformers with two hindered methoxy groups than for the other form because electron donation to the ring is stronger if the $O-CH_3$ bond is in plane with the ring. This difference in midpoint potential could extend up to ∼70 mV. The difference in redox potentials between two quinones in bacterial reaction center were proposed to relate to differences in the methoxy group conformations (*27*). The possible influence of the protein environment on the midpoint potential of the bound ubiquinone may be crucial for turnover at the Q_H and Q_L sites of quinol oxidases.

C═C Modes of the Neutral Bound Quinone. The C═C modes of the bound ubiquinone can be assigned to the 1612 cm^{-1} band in the double difference spectrum (Figure 4a). They are primarily unaffected upon binding, as confirmed by the C═C modes in the spectra of the ^{13}C-labeled forms (Figure 4b,c), essentially corresponding to the signals observed for the free forms. Due to several overlapping signals in the 1634−1600 cm^{-1} region, the small shifts upon ^{13}C labeling were difficult to analyze.

Modes of the Methoxy Group of the Neutral Bound Quinone. The signals of the $C-OCH_3$ mode from the 2- and 3-methoxy groups can be seen at 1288 and 1266 cm^{-1} (Figure 4), as described above for the quinones in solution (Figures 1 and 2). The shifts do not exceed 2 cm^{-1}; thus, no strong interactions exist. The $C-OCH_3$ mode shows no alteration, independent from the present $CO-CH_3$ conformer discussed. In the double difference spectra (Figure 4) a difference signal at 1452 cm^{-1} can be seen. This signal was assigned to the vibrational modes of the methyl side groups of ubiquinone before (see Figure 1) and indicates some anchoring of the side chains in the binding pocket.

Modes of the Reduced Bound Quinone. The difference signals of the unlabeled UQ_2H_2 can be identified at 1490,

1470, 1430, and 1390 cm^{-1} (Figure 4a) and are comparable to those in Figure 2. Only negligible shifts from the modes of the quinone ring were found. The ubisemiquinone anion form that would yield a very strong signal at ~1484 cm^{-1}, with the position depending on hydrogen bonding, was not observed. This can be attributed to the conditions applied, predominantly to the long equilibration of the sample, leading to the immediate protonation of the semiquinone anion ($Q^{-\bullet}$) that reacts further to UQ_2H_2.

Difference Signals Reflecting Alterations in the Protein upon Quinone Binding. In Figure 4, difference signals can be observed that cannot be attributed to quinone modes and seem to reflect alterations in the protein upon quinone binding. Assignments of the modes at 1706, 1684, and 1676 cm^{-1} to C═O modes of protonated COOH groups (heme propionates, Asp or Glu side chains), C═O modes of Asn or Gln side chains, or the $\nu_{as}(CN_3H_5)$ of Arg are conceivable (*34*). Additional assignments can be made to the reorganization of secondary structure elements. Between 1700 and 1670 cm^{-1} contributions from β-sheet structures and loops can be expected, and the strong negative signals between 1646 and 1636 cm^{-1} (Figure 4) may reflect the reorganization of β-sheet structures (*35*). Furthermore, a contribution from the $\nu_s(CN_3H_5)$ mode of Arg may be related to this signal, on the basis of absorption spectra of isolated Arg (*34*).

A difference signal at 1540 cm^{-1} is observed in the double difference spectra (Figure 4) and can be tentatively assigned to the C═C modes of the porphyrin ring on the basis of model compound studies of heme B (*36*) and comparison with other oxidases (*37*). A previous resonance Raman study showed that ubiquinone binding affects the porphyrin modes of oxidized low-spin heme *b* (*4*). The signal observed here for the reduced form may be interpreted in this sense, presuming that the quinone interacts with the porphyrin ring of heme *b*. An alternative assignment of this signal to amide II modes is less probable, since upon H/D exchange no characteristic shift of this signal was observed (data not shown). However, the antisymmetric COO^- modes from heme propionates in cytochrome *c* oxidase from *P. denitrificans* have been reported to contribute between 1570 and 1524 cm^{-1} (*38*). The interaction between a deprotonated heme propionate and the bound quinone, or a change in the protonation state, may lead to these additional difference signals.

As described above, the difference signal at 1452 cm^{-1} can be assumed to arise from the $\delta_{as}(CH_3)$ of the ubiquinone. Alternatively, this signal may be attributed to the ν(CC), ν(CN), and δ(CH) modes from Trp (*38*) or the $\nu_S COO^-$ vibrations of deprotonated Asp or Glu side chains.

Electrochemically Induced FTIR Difference Spectra of Wild-Type Cytochrome bo_3 from E. coli with Bound UQ_8. Figure 5 shows the electrochemically induced FTIR difference spectrum of the cytochrome bo_3 with bound UQ_8 isolated from the wild-type strain for a potential step from −0.5 to 0.5 V. On the basis of the experiments described above, characteristic ubiquinone/ubiquinol modes can be clearly identified. For the neutral UQ_8 (positive bands), the ν(C═O) and ν(C═C) modes were assigned at 1656 and 1612 cm^{-1}, respectively. Other characteristic signals can be observed at 1286, 1264, and 1204 cm^{-1}. The bands for the UQ_8H_2 (negative signals) can be observed at 1390, 1470, and 1488 cm^{-1}. The native ubiquinone in the cytochrome

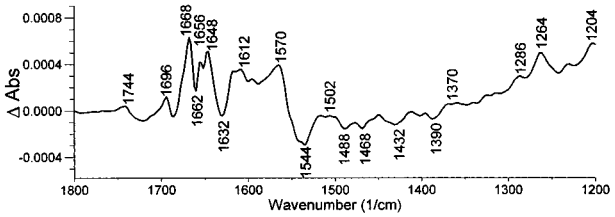

FIGURE 5: Oxidized minus reduced FTIR difference spectra of cytochrome bo_3 from *E. coli* for a potential step from −0.5 to 0.5 V.

bo_3 from *E. coli* is an ubiquinone 8 with six additional isoprene units. A comparison of the difference signals of UQ_8 with the signals assigned to UQ_2 should demonstrate the influence of the number of isoprenyl units on the absorption of the C═O and C═C modes. It has been reported for UQ_1, UQ_{10} (*26*), and UQ_8 (*16*) that the influence does not lead to shifts larger than 2 cm^{-1}. However, the shoulder at 1664 cm^{-1} in the absorbance spectra of UQ_1−UQ_{10} is more intense with respect to the increasing number of isoprenyl units.

One important question is to determine whether the quinone signals arise from quinone tightly bound within the binding pocket or from quinones in detergent micelles. A clear indication for the former is a sharp signal at 1656 cm^{-1} for the ν(C═O) mode (Figure 5), which changed to a broad signal at 1650 cm^{-1} in a free form (Figure 2). This is consistent with the shift observed for UQ_2 bound to ΔUbiA (see Figure 3b). FTIR spectroscopy can thus be used to determine the presence of the tightly bound ubiquinone at the Q_H site of cytochrome bo_3 where the ubiquinone content considerably varies depending on the purification procedure (*4*). On the basis of the signal intensity of the ubiquinone mode in relation to the protein modes, the occupancy of the Q_H site with UQ_8 in the preparation used for the experiments shown in Figure 5 clearly exceeds 60%. The difference signals indicating alterations in the protein upon ubiquinone binding (Figure 3b) are also present in the UQ_8-bound cytochrome bo_3 (Figure 5). The presumed heme C═C mode, for example, can be seen at 1544 cm^{-1}, as shown for the ΔUbiA reconstituted with UQ_2 (Figure 3b).

CONCLUSIONS

Selective ^{13}C-labeling of the bound ubiquinone in cytochrome bo_3 offers the possibility to identify the vibrational modes of the ubiquinone in situ. On the basis of the experiments with the specifically ^{13}C-labeled UQ_2 analogues, both C═O modes could be distinguished and the mainly symmetrical binding of the ring portion to the binding pocket was revealed. An essentially weak hydrogen bonding of the two ubiquinone C═O groups with the protein was found. By comparison of the infrared data with semiempirical calculations (*27*), the 3-methoxy group appears to be free from steric constraints and the 2-methoxy group appears to be hindered. This is in agreement with a previous structure−function study revealing the importance of the 2-methoxy and the 5-methyl group for the catalytic turnover (*19*). An important part of this study relates to alterations in the protein moiety upon ubiquinone binding, evident by a number of bands in the electrochemically induced FTIR difference spectra that are not ubiquinone vibrational modes. For a more detailed analysis of the effects of ubiquinone binding on the

vibrational modes of the protein, combined infrared and mutagenesis studies will be necessary for the identification of amino acid residues participating in ubiquinone/ubiquinol binding in cytochrome bo_3 and in its redox and protonation reactions.

ACKNOWLEDGMENT

We thank Christine Ernd for excellent technical assistance.

REFERENCES

1. Calhoun, M. W., Thomas, J. W., and Gennis, R. B. (1994) *Trends Biochem. Sci. 19*, 325−330.
2. Garcia-Horsman, J. A., Barquera, B., Rumbley, J., Ma, J., and Gennis, R. B. (1994) *J. Bacteriol. 176*, 5587−5600.
3. Mogi, T., Tsubaki, M., Hori, H., Miyoshi, H., Nakamura, H., and Anraku, Y. (1998) *J. Biochem. Mol. Biol. Biophys. 2*, 79−110.
4. Sato-Watanabe, M., Mogi, T., Ogura, T., Kitagawa, T., Miyoshi, H., Iwamura, H., and Yasuhiro, A. (1994) *J. Biol. Chem. 269*, 28908−28912.
5. Sato-Watanabe, M., Itoh, S., Mogi, T., Matsuura, K., Miyoshi, H., and Anraku, Y. (1995) *FEBS Lett. 374*, 265−269.
6. Ingledew, W. J., Ohnishi, T., and Salerno, J. C. (1995) *Eur. J. Biochem. 227*, 903−908.
7. Welter, R., Gu, C. Q., Yu, L., Yu, C.-A., Rumbley, J. N., and Gennis, R. B. (1994) *J. Biol. Chem. 269*, 28834−28838.
8. Puustinen, A., Verkhovsky, M., Morgan, J. L, Bevevich, N. P., and Wikström, M. (1996) *Proc. Natl. Acad. Sci. U.S.A. 93*, 1545−1548.
9. Sato-Watanabe, M., Mogi, T., Miyoshi, H., and Anraku, Y. (1998) *Biochemistry 37*, 5356−5361.
10. Sato-Watanabe, M., Mogi, T., Sakamoto, K., Miyoshi, H., and Anraku, Y. (1998) *Biochemistry 37*, 12744−12752.
11. Tsatsos, P. H., Reynolds, K., Nickels, E. F., He, D.-Y, Yu, C.-A., and Gennis, R. B. (1998) *Biochemistry 37*, 9884−9888.
12. Ma, J., Puustinen, A., Wikström. M., and Gennis, R. B. (1998) *Biochemistry 37*, 11806−11811.
13. Thibodeau, D. L., Breton, J., Berthomieu, C., Bagley, K. A., Mäntele, W., and Nabedryk, E. (1990) in *Reaction Centers of Photosynthetic Bacteria* (Michel-Beyerle, M.-E., Ed.) pp 87−98, Springer-Verlag, Berlin.
14. Breton, J., Boullais, C., Berger, G., Mioskowski, C., and Nabedryk, E. (1995) *Biochemistry 34*, 11606−16.
15. Breton, J., Boullais, C., Burie, J. R., Nabedryk, E., and Mioskowski, C. (1994) *Biochemistry 33*, 14378−86.
16. Breton, J., Burie, J. R., Berthomieu, C., Berger, G., and Nabedryk, E. (1994) *Biochemistry 33*, 4953−65.
17. Breton, J., Burie, J. R., Boullais, C., Berger, G., and Nabedryk, E. (1994) *Biochemistry 33*, 12405−15.
18. Breton, J., Thibodeau, D. L., Berthomieu, C., Mäntele, W., Vermeglio, A., and Nabedryk, E. (1991) *FEBS Lett. 278*, 257−260.
19. Sakamoto, K., Miyoshi, H., Takegami, K., Mogi, T., Anraku, Y., and Iwamoto, H. (1996) *J. Biol. Chem. 271*, 29897−29902.
20. Sakamoto, K., Miyoshi, H., Ohshima, M., Kuwabara, K., Kano, K., Akagi, T., Mogi, T., and Iwamoto, H. (1998) *Biochemistry 37*, 15106−15113
21. Sato-Watanabe, M., Mogi, T., Miyoshi, H., Iwamura, H., Matsushita, K., Adachi, O., and Anraku, Y. (1994) *J. Biol. Chem. 269*, 28899−28907.
22. van Liemt, W. B. S., Steggerda, W. F., and Lugtenburg, J. (1994) *Recl. Trav. Chim. Pays-Bas 113*, 153−161.
23. Tsubaki, M., Mogi, T., Anraku, Y., and Hori, H. (1993) *Biochemistry 32*, 6065−6072.
24. Rumbley, J. N., Nickels, E. F., and Gennis, R. B. (1997) *Biochim. Biophys. Acta 1340*, 131−142.
25. Moss, D. A., Nabedryk, E., Breton, J., and Mäntele, W. (1990) *Eur. J. Biochem. 187*, 565−572.
26. Hellwig, P., Behr, J., Ostermeier, C., Richter, O.-M. H., Pfitzner, U., Odenwald, A., Ludwig, B., Michel, H., and Mäntele, W. (1998) *Biochemistry 37*, 7390−7399.
27. Burie, J. R., Boullais, C., Nonella, M., Mioskowski, C., Nabedryk, E., and Breton, J. (1997) *J. Phys. Chem. 101*, 6607−6617.
28. Boullais, C., Nabedryk, E., Burie, J. R., Nonella, M., Mioskowski, C., and Breton, J. (1998) *Photosynth. Res. 55*, 247−252.
29. Bauscher, M., and Mäntele, W. (1992) *J. Am. Chem. Soc. 96*, 1101−1108.
30. Puustinen, A., Bailey, J. A., Dyer, R. B., Mecklenburg, S. L., Wikström, M., and Woodruff, W. H. (1997) *Biochemistry 36*, 13195−13200.
31. Yamazaki, Y., Kandori, H., and Mogi, T. (1999) *J. Biochem. (Tokyo)* (in press).
32. Lübben, M., Prutsch, A., Mamat, B., and Gerwert, K. (1999) *Biochemistry 38*, 2048−56.
33. Prince, R. C., Dutton, P. L., and Bruce, J. M. (1983) *FEBS Lett. 160*, 273−276.
34. Venyaminov, S. Y., and Kalnin, N. N. (1990) *Biopolymers 30*, 1272.
35. Arrondo, J. L. R., Muga, A., Castresana, J., and Goni, F. M. (1993) *Prog. Biophys. Mol. Biol. 59*, 23−56.
36. Berthomieu, C., Boussac, A., Mäntele, W., Breton, J., and Nabedryk, E. (1992) *Biochemistry 31*, 11460−11471.
37. Hellwig, P., Grzybek S., Behr, J., Ludwig, B., Michel, H., and Mäntele, W. (1999) *Biochemistry 38*, 1685−1694.
38. Behr, J., Hellwig, P., Mäntele, W., and Michel, H. (1998) *Biochemistry 37*, 7400−7406.
39. Takeuchi, H., and Harda, I. (1986) *Spectrochim. Acta A42*, 1069−1078.

BI991267H